The effect of substrate modulus on the growth and function of matrix-embedded endothelial cells

Citation: Murikipudi, Sylaja, Heiko Methe, and Elazer R. Edelman. "The Effect of Substrate Modulus on the Growth and Function of Matrix-Embedded Endothelial Cells." Biomaterials 34, no. 3 (January 2013): 677–684.

As Published: http://dx.doi.org/10.1016/j.biomaterials.2012.09.079

Publisher: Elsevier

Persistent URL: http://hdl.handle.net/1721.1/102307

Version: Author's final manuscript: final author's manuscript post peer review, without publisher's formatting or copy editing

Published in final edited form as:
Biomaterials. 2013 January ; 34(3): 677–684. doi:10.1016/j.biomaterials.2012.09.079.

The effect of substrate modulus on the growth and function of matrix-embedded endothelial cells

Sylaja Murikipudi[a,*], **Heiko Methe**[a,b,#], and **Elazer R. Edelman**[a,%]

[a]Harvard-MIT Division of Health Sciences and Technology, Massachusetts Institute of Technology, Cambridge, Massachusetts 02139

[b]Department of Internal Medicine/Cardiology, University Hospital Grosshadern, Ludwig-Maximilians-University Munich, Marchioninistrasse 15, 81377 Munich, Germany

Abstract

Endothelial cells (EC) are potent bioregulatory cells, modulating thrombosis, inflammation and control over mural smooth muscle cells and vascular health. The biochemical roles of EC are retained when cells are embedded within three-dimensional (3D) denatured collagen matrices. Though substrate mechanics have long been known to affect cellular morphology and function and 3D-EC systems are increasingly used as therapeutic modalities little is known about the effect of substrate mechanics on EC in these 3D systems. In this work, we examined the effect of isolated changes in modulus on EC growth and morphology, extracellular matrix gene expression, modulation of smooth muscle cell growth, and immunogenicity. EC growth, but not morphology was dependent on scaffold modulus. Increased scaffold modulus reduced secretion of smooth muscle cell growth inhibiting heparan sulfate proteoglycans (HSPGs), but had no effect on secreted growth factors, resulting in a loss of smooth muscle cell growth inhibition by EC on high modulus scaffolds. Expression of ICAM-1, VCAM-1 and induction of $CD4^+$ T-cell proliferation was reduced by increased scaffold modulus, and correlated with changes in integrin α5 expression. Expression of several common ECM proteins by EC on stiffer substrates dropped, including collagen IV(α1), collagen IV(α5), fibronectin, HSPGs (perlecan and biglycan). In contrast, expression of elastin and TIMPs were increased. This work shows even modest changes in substrate modulus can have a significant impact on EC function in three-dimensional systems. The mechanism of these changes is not clear, but the data presented herewithin suggests a model wherein EC attempt to neutralize changes in environmental force balance by altering ECM and integrin expression, leading to changes in effects on downstream signaling and function.

Keywords

matrix-embedded endothelial cells; gelatin scaffold; modulus; smooth muscle growth inhibition; inflammation

*Corresponding author, sylajam@mit.edu, phone: 617-253-1569.
#hmethe@mit.edu
%ere@mit.edu

7. DISCLOSURES

None

1. INTRODUCTION

Substrate mechanics have long been known to affect both cellular morphology and function. Many cell types spread more on stiffer substrates [1–4] or migrate towards regions of stiffer substratum [2,5–7]. Properties of fibroblasts, smooth muscle cells and chondrocytes, including focal adhesion formation [1,8], tyrosine signaling [8,9], and proliferation [10–12] are all affected by substrate mechanics across both 2D and 3D culture. Cell-specific functions of e.g. hepatocytes, mammary epithelial cells, and spinal neurons are also affected by substrate rigidity. [13–15]

The question of how substrate rigidity affects endothelial cell (EC) function is of importance as many diseases, such as atherosclerosis and hypertension [16,17], are associated with altered vessel mechanical properties. EC create a semi-permeable tubular lining. These powerful and dynamic cells sense and then respond to flow from above, pressure from below, and neighboring cell density at their periphery - secreting a full spectrum of bioactive compounds in a manner sensitive to cell state and environmental cues [18–20]. Changes in mechanical properties have also been linked to alterations in EC gene expression associated with altered extracellular matrix deposition, integrin expression and cell signaling. [21] Most studies using EC have looked at the effect of 2D substrate mechanics on the *physical* state of the cells, rather than their functionality. Changes in substrate mechanics affect migration [5], spreading, stress fiber formation [1, 22, 23], focal adhesions, and integrin expression [22]. As 3D constructs are increasingly appreciated for clinical potential [24–36] and 3D niches for EC are being identified, these studies of EC physical state are being extended into 3D culture. Endothelial tubulogenesis is increased in softer 3D gels compared to stiffer ones, with differing morphology [37–40]. Changes in focal adhesion composition were also seen. [40] However, there is far less in the literature on the effect of 3D substrate mechanics on the *function* of EC.

We examined biology of EC embedded within 3D biodegradable matrices of denatured collagen of variable stiffness. These materials have served as scaffold supporting EC growth effectively controlling intimal hyperplasia after vascular manipulation, [24–26] and in the setting of arterio-venous fistula creation for dialysis access in animal [26,27] and human trials. [28]. Although these constructs have been very effective and display an additional interesting ability to modulate the immune response [29–34], allowing use of allogenic or even xenogenic EC, it may be possible to improve their performance. Knowing how the scaffold's physical and mechanical properties affect EC function may allow for further optimization of tissue engineered systems in addition to offering valuable insights into EC biology in health and disease.

2. MATERIALS AND METHODS

2.1 Gelatin Scaffold Preparation

Gelatin scaffolds of varying modulus were created by modifying a commercially available gelatin surgical sponge (Gelfoam). Scaffolds of increased stiffness were created by incubating Gelfoam in a sterile solution of 1-ethyl-3-(3-dimethylaminopropyl)carbodiimide hydrochloride (EDAC, EMD Biosciences) and *N*-hydroxysuccinimide (non-persistent crosslinkers which create amide bonds between existing amine and carboxyl groups without incorporation into the scaffold) [41,42] (NHS, Thermo Scientific) in PBS twice for 1.5 hours at room temperature with shaking, followed by 4, 15 minute washes with sterile PBS to remove any residual crosslinker. The concentrations of EDAC and NHS were varied (54.0/22.0, 36.1/14.6, 9.0/3.6, 3.6/1.4 EDAC/NHS mM) to create different degrees of cross-linking, and therefore different degrees of stiffness. Scaffolds of reduced stiffness were

created by heating Gelfoam in PBS for either 10 or 20 minutes at 121°C, 20mmHg using an autoclave. Scaffolds were stored in sterile PBS at 4°C until use.

2.2 Scaffold Mechanical Property Characterization

Scaffold stiffness was characterized by uniaxial compression of 12mm scaffold disks using a Zwick mechanical tester. Scaffolds were immersed in a PBS bath and compressed at a rate of 0.01mm/s. Resulting stress-strain curves were typical of unconfined compression of porous solids, with a “toe” region, a region of linear slope where Young’s modulus was measured, and a sharp, asymptotic increase in slope thereafter.

2.3 Endothelial Cell Culture and Scaffold Engraftment

Human aortic EC (HAEC) from three healthy donors were purchased from Promocell, pooled and used from passages 5–8. Prior to scaffold engraftment, and for 2D controls, cells were cultured on gelatin coated (0.1%, 30 minutes) culture dishes. For culture in scaffolds, HAEC were trypsinized, resuspended at 1×10^6 cells/mL in culture media and pipetted evenly onto scaffolds at a density of ~3.6×10^4 cells/cm^2. Experiments were generally conducted using 1.5cm^2 scaffolds, except for measurement of cell growth rate, which utilized cells recovered from 8mm scaffold discs. After seeding, scaffolds were incubated for 3 hours at 37°C, transferred to 30mL polypropylene tubes with culture media (ECGM2 [Promocell], supplemented with 7% FBS and antibiotics) and incubated at 37°C, 5% CO_2. For experiments requiring free cells, cells were recovered by digestion in collagenase IV in 1:1 ECGM2:PBS at 37°C. After gelatin scaffolds were completely digested, cells were recovered by centrifugation.

To determine cell growth, 3–8mm scaffolds of each type were harvested on days 0, 2, 5, 8, 12, 16, 21 and 28 and counted using a Coulter Counter. Growth rate for each scaffold type was determined to be the slope of the linear regression of the cell number vs. time curve during the growth phase (days 5–21).

2.4 Scaffold Staining and Visualization

Scaffolds were cultured for the desired period of time, rinsed with PBS and fixed with 4% paraformaldehyde overnight at 4°C. All subsequent steps were carried out on ice or at 4°C. Following fixation, scaffolds were washed thrice for 5 minutes with PBS followed by a 10 minute incubation with 200mM glycine in PBS. Scaffolds were again washed thrice for 5 minutes with PBS and then transferred to ice cold 18% w/v sucrose in PBS for 3 hours, followed by ice cold 30% w/v sucrose in PBS for an additional 3 hours. Scaffolds were then washed thoroughly with PBS and flash frozen with liquid nitrogen.[43] Sections with a thickness of 20–60μm were cut using a cryotome and captured on positively charged slides (SuperFrost Plus, VWR). Sections were stored at −80°C for up to 3 weeks before staining.

Slides were allowed to reach room temperature, washed twice with PBS and then permeabilized with 0.2% Triton X-100 in PBS for 10 minutes. Sections were blocked for 1 hour in 1% BSA + 20% goat serum in PBS. Sections were immediately incubated in 1:50, mouse anti-porcine CD31 (Serotec) in 1%BSA/PBS overnight at 4°C in a humidified chamber. Sections were washed 3x five minutes with 1%BSA/PBS and incubated 1 hour in the dark at room temperature with Alexa 488 conjugated goat anti-mouse IgG, 1:75 (Invitrogen) in 1%BSA/PBS containing rhodamine phalloidin. Sections were washed thrice for five minutes with PBS and coverslipped using fade resistant mounting medium containing DAPI (Vectashield with DAPI, Vector). Stained samples were stored in the dark at 4°C until imaged.

Staining was visualized using a Perkin-Elmer spinning disk confocal microscope at 63X magnification with an oil immersion lens. Samples were imaged at z-intervals of 1μm. the resulting z-stack was turned into a maximal intensity z-projection image using ImageJ software. For quantification of actin staining intensity, samples were imaged using a Zeiss LSM 510 confocal microscope at 40X magnification with a water immersion lens. Average pixel intensity of each image was quantified using ImageJ. The average of 10, 40x fields was used to calculate actin staining intensity for each scaffold type.

2.5 Endothelial Cell Conditioned Media Preparation and Characterization

Confluent scaffolds were washed with serum free medium thrice for 10 minutes. For growth factor or glycosaminoglycan measurement, scaffolds were incubated in 3.5mL EC basal medium 2 (ECBM2, Promocell) supplemented with 0.5% FBS and antibiotics for 24 hours. For measurement of inflammatory cytokines, scaffolds were incubated in 10mL complete growth media (Endothelial Cell Growth Medium + 7% FBS + 1% PS) supplemented with 10ng/mL TNF-α for 24 hours. Conditioned medium was collected, centrifuged to remove any particulates, and frozen at −80°C until use. Cells were recovered from scaffolds and counted using a Coulter Counter.

Low serum conditioned media was assayed for TGF-β1, FGF2, and PDGF using ELISAs from R&D according to kit directions. Concentrations of IL-6, IL-8 and MCP-1, in conditioned media containing full growth supplements plus TNF-α prepared as described above, were also measured using ELISAs from R&D according to kit directions. Total glycosaminoglycan and heparan sulfate proteoglycan (HSPG) in low serum conditioned media was measured using a dimethylmethylene blue (DMB) assay. Conditioned media was concentrated 2 fold using 3000 MWCO centrifugal concentrators (Millipore). DMB assay solution was prepared according to the method of Farndale et. al.[44] To determine the total amount of GAG in samples, 700μl DMB was added to a 500μl sample and absorbance was immediately read at 523 nm using a spectrophotometer (Perkin-Elmer) and compared to a standard curve prepared using chondroitin sulfate in ECBM2 + 0.5% FBS + PS. To determine the amount of HSPG in the samples, conditioned media was digested with 0.036U/mL protease-free chondroitinase ABC for 3 h at 37°C prior to measurement of GAG with DMB. The GAG remaining after digestion was considered to be the HSPG fraction. All samples were measured with and without chondroitinase digestion, in duplicate.

2.6 Smooth Muscle Culture and Growth Inhibition

Human aortic smooth muscle cells (HASMCs) were purchased from Promocell and cultured in DMEM supplemented with 5% calf serum (CS) and 1% PSG. For inhibition experiments, HASMCs were sparsely seeded in 48 well plates (3.75×10^3 per well), allowed to attach overnight and then starved for 24 hours with DMEM supplemented with 0.1% CS and PS. Following starvation, culture medium was replaced with either EC conditioned medium (n = 3, in duplicate) or fresh ECBM2+0.5% FBS+PS (n = 3, in duplicate) and all wells then adjusted to 5% total serum. After 24 hours, to measure proliferation, ^{3}H-thymidine was added to each well to a concentration of 1mCi/μL and cells incubated an additional 6 hours. Cells were then washed 3x with ice cold PBS followed by incubation with 10% trichloroacteic acid in PBS for 30 minutes at 4°C. Cells were washed twice with 95% ethanol and solubilized with 0.1% SDS in 0.25N NaOH. Samples were transferred to scintillation vials with UltimaGold cocktail and ^{3}H-thymidine incorporation measured using BD LSC and QuantaSmart software. Results were expressed as percent decrease in ^{3}H-thymidine incorporation vs. control medium, either per scaffold or normalized to EC number.

2.7 Allogeneic T Cell Proliferation Assay

EC were cultured on scaffolds under normal culture conditions for 16 days and then exposed to 1000U/mL IFN-γ for 48 hours. Cell growth was subsequently arrested using 50μg/mL mitomycin C. $CD4^+$ T cells were isolated from fresh human blood using a negative selection kit (Miltenyi). Isolated T cells were labeled with 10μM carboxyfluorescein succinimidyl ester (CFSE, Invitrogen) for 10 minutes at 37°C in phenol red free RPMI1640, and washed three times. Labeled $CD4^+$ T cells were co-cultured with scaffolds at 5×10^5 T cells per 1.25×10^5 EC (in triplicate for each scaffold type) or with empty scaffolds, in RPMI medium without phenol red, and maintained for six days. At the end of the co-culture period, scaffolds were washed extensively, and T cells pelleted by centrifugation. T cells were resuspended in PBS and analyzed by flow cytometry. Proliferation (i.e. division) of T cells resulted in less intense staining per cell and decrease in mean fluorescence intensity of the cells.

2.12 Flow Cytometry

EC were recovered from scaffolds after reaching confluence. (For determination of inflammatory receptor expression, 10ng/ml TNF-α was added to culture medium for 24 hours before recovery.) Cells were washed with FACS buffer (PBS with 2% heat inactivated FBS and 0.1% sodium azide, BD Biosciences) and incubated with FITC labeled mouse anti-human ICAM-1 or mouse anti-human VCAM-1 diluted in FACS buffer for 45 minutes on ice. Cells were washed twice with FACS buffer and fixed with 1% paraformaldehyde in PBS. 10^4 cells were then analyzed by flow cytometry using a FACScalibur intstrument and CellQuest Pro software (Becton Dickinson, San Diego, CA).

2.13 RT-PCR

After 21 days of culture, soft (20 minutes Autoclave), unmodified Gelfoam and stiff (54.0/22.0 EDAC/NHS mM) scaffolds were rinsed with PBS, flash frozen and cut into thin sections using a cryotome to reduce scaffold volume and simplify RNA extraction. All sections from an individual scaffold were pooled and total RNA was extracted (RNeasy Mini Kit, Qiagen, Valencia, CA).Complementary DNA was synthesized using the TaqMan reverse transcription reagents from Applied Biosystems (Foster City, CA). Real-time PCR analysis was performed with an Opticon Real Time PCR Machine (MJ Research) using SYBR Green PCR Master Mix Reagent Kit (Applied Biosystems). Primers for extracellular matrix genes were designed using Primer3 and purchased from Invitrogen (Supplemental Data, Table 1).

2.14 Statistics

Statistical analyses were performed with Prism (GraphPad) or Excel (Microsoft) software. Data are expressed as mean±SEM unless noted. Comparisons between groups were made by ANOVA followed by Tukey's multiple comparison test. A value of $p < 0.05$ was considered statistically significant.

3. RESULTS

3.1 Scaffold Modulus

Scaffold modulus depends on crosslinking ($p < 0.0001$ by ANOVA, Fig. 1). The hydrated modulus of unmodified Gelfoam (173±5.9Pa) could be reduced almost 3.5 fold to 50±9.6Pa by 20 minutes of heating in PBS at 121°C, 20mmHg ("Soft" scaffold) and increased almost 8 fold to 1345±34.5Pa by treatment with 54.0/22.0 EDAC/NHS mM solution ("Stiff" scaffold). The increase in scaffold modulus with EDAC/NHS treatment was linearly related ($r^2=0.98$, $p<0.0001$) to the concentration of cross-linker used.

3.2 Growth rate but not Cell Morphology or Secretion is Scaffold Modulus-Dependent

EC on all scaffolds formed islands of cobblestone-like morphology, reaching confluence by ~21 days, and expressing a normal pattern of EC markers, including CD31 (Figure 2). Growth rate, as well as cell number at confluence, varied with scaffold modulus ($p < 0.0001$). Growth rate and cell number were highest on scaffolds of intermediate stiffness, falling off at softer and stiffer moduli. Maximum growth rate and cell number at 508Pa statistically differed from growth rate and cell number on the stiffest and softest scaffolds (Figure 3, $p < 0.05$). In contrast actin cytoskeleton morphology was visually similar on scaffolds of different modulus, with stress fibers visible in all cells on all scaffolds. Staining intensity did not vary between scaffold types.

3.3 Extracellular Matrix Protein Gene Expression

Extracellular matrix (ECM) protein and remodeling gene expression was examined by RT-PCR. Several ECM genes were downregulated on 1345Pa scaffolds vs. 50Pa scaffolds ($p < 0.05$) including collagen IV(α1) (COL4A1) (0.34±0.12 vs. 1±0.13, copy number normalized to 50Pa scaffolds), collagen IV(α5) (COL4A5) (0.33±0.08 vs. 1±0.12), fibronectin (FN1) (0.26±0.06 vs. 1±0.1), perlecan (i.e. HSPG) (0.22±0.06 vs. 1±0.24) and biglycan (BGN) (0.18±0.07 vs. 1±0.13). Other structural genes, including collagen IV(α6), collagen III(α1), collagen I(α1) and laminin were unaffected (Supplemental Data Figure 1). When it did change, expression for all genes changed in concert, with the exception of those genes most associated with matrix elasticity. Elastin expression rose on 1345Pa scaffolds compared to 173Pa scaffolds (2.56±0.76 vs. 0.77±0.12) and continued to trend lower on 50Pa scaffolds, while, similarly, fibrillin expression was downregulated on 1345Pa vs. 50Pa scaffolds (0.47±0.16 vs. 1±0.09).

It is also of note that the *ratio* of change in expression of elastin relative to structural COLIV(α1) expression increased significantly with modulus, rising almost 7-fold in EC on 1345Pa scaffolds when compared to EC on 50Pa scaffolds ($p < 0.01$).

Expression of remodeling genes followed the same pattern observed for proliferation and inflammation – genes coding for proteins that *stimulate* remodeling such as MMP-2 and MTI-MMP were unchanged with modulus while *inhibitors* of matrix metalloproteinases like TIMP-1 and TIMP-2 increased on 1345Pa scaffolds vs. 173Pa scaffolds (1.53±0.27 vs. 0.55±0.07 and 1.88±0.27 vs. 0.78±0.09 respectively).

3.4 Integrin Expression

Integrin $\alpha_5\beta_1$ expression was dependent on scaffold stiffness. Expression of integrin subunit genes ITGA5 and ITGB1 was lower on stiffer scaffolds (1345Pa and 173Pa vs. 50Pa ($p < 0.05$), and 1345Pa vs. 50Pa ($p < 0.05$) respectively). Lower expression was confirmed by flow cytometry. Integrin α_5 was expressed by 100% of cells, but geometric mean of fluorescence correlated with scaffold stiffness with fluorescence linearly decreasing from 524.3±5.5 at 50Pa to 252.3±1.4 at 1345Pa ($r^2 = 0.90$). No statistically significant differences were seen in integrin $\alpha_v\beta_3$ subunit gene (ITGAV and ITGB3) expression. Similarly, although flow cytometry showed a small (Δ_{max} of ~17%) but significant ($p < 0.0001$) drop in integrin $\alpha_v\beta_3$ surface expression with increased stiffness, no difference was seen in the geometric mean of fluorescence, suggesting similar levels of expression in all cells. (See Supplemental Figure 2)

3.5 Inhibition of Smooth Muscle Cell Proliferation

EC inhibit smooth muscle cell proliferation when the former are confluent and quiescent, and promote SMC growth when EC are in their growth phase or dysfunctional [18]. Smooth muscle cell inhibition by conditioned media from matrix-embedded EC, expressed as

fractional decrease in ^{3}H-thymidine incorporation per 10^6 ECs, was strongly dependent on scaffold modulus at low moduli (Figure 4, $p < 0.0004$ by ANOVA over entire scaffold range), though it plateaued at higher moduli. Inhibition was maximal at the lowest modulus, 50Pa (0.975±0.383), and decreased with modulus until minimal inhibition was reached at 508Pa (0.200±006). At maximum inhibition smooth muscle ^{3}H-thymidine incorporation was reduced by 97.5±22.1%, consistent with the optimum function of quiescent EC. Inhibition was linearly related to HSPG secretion (Figure 4, $r^2 = 0.80$) but not to the expression and secretion of growth factors. Growth factor release was largely unaffected by scaffold modulus. TGF-β1 secretion ranged from 2289±213 ng/10^6 cells (at 1345Pa) to 2826±319 ng/10^6 cells (at 376Pa) but did not differ significantly with scaffold modulus. PDGF-BB secretion ranged from 123±15 pg/10^6 cells (at 173Pa, unmodified Gelfoam) to 230±21 pg/10^6 cells (at 1062Pa). FGF2 secretion ranged from 180±6.9 pg/10^6 cells (at 68.7Pa) to 364±23 pg/10^6 cells (at 1062Pa).

3.6 Immunogenicity of Endothelial Cells is Partially Modulus-Dependent

3-D matrix-embedded EC exert an immunodulatory function [29]. Endothelial expression of adhesion molecules in response to TNFα stimulation varied inversely with scaffold modulus. ICAM-1 was expressed by 51.8±4.2% of cells at 50Pa, decreasing linearly to 31.3±5.7% at 1345Pa. VCAM-1 was expressed by 18.8±0.3% of cells at 50Pa, monotonically decreasing to 1.6±0.6% at 1345Pa. Both ICAM-1 and VCAM-1 expression linearly correlated with cell surface integrin α_5 expression ($r^2 = 0.80$ and $r^2 = 0.78$ respectively, data not shown).

In contrast, secretion of proinflammatory cytokines (MCP-1, IL-6 and IL-8) was largely unaffected by 3D scaffold modulus. EC stressed on tissue culture polystyrene plates express significant levels of MCP-1, IL-6 and IL-8 (13.37±0.79 ng/10^6 cells, 221.2±66.4 ng/10^6 cells and 746.5±97.4 ng/10^6 cells respectively). EC in denatured three-dimensional matrices secreted far less of all of these cytokines. MCP-1 secretion ranged from 3.05±0.83 ng/10^6 cells (at 50Pa) to 3.76±0.51 ng/10^6 cells (at 1345Pa), IL-6 secretion ranged from 9.49±1.86 ng/10^6 cells (at 508Pa) to 16.2±3.62 ng/10^6 cells (at 50Pa), and IL-8 secretion ranged from 104±6.1 ng/10^6 cells (at 508Pa) to 142.4±12.9 ng/10^6 cells (at 1345Pa). Dependence of secretion on modulus was not statistically significant except for IL-6 ($p = 0.02$ by ANOVA), where absolute differences in secretion were small, and did not differ significantly.

As we have previously demonstrated attenuated proliferation of allogeneic T cells exposed to matrix-embedded EC when compared with EC cultured on tissue culture polystyrene plates we next assayed the effect of 3D modulus on allogeneic T cell proliferation by CFSE-staining. Mean fluorescence intensity (MFI) of T cells is inversely proportional to T-cell proliferation, and increased with scaffold modulus, indicating a greater proliferation of T cells in the presence of softer scaffolds (Figure 5a). MFI ranged from 65.9±4.8 at 50Pa to 153.7±4.7 at 1345Pa. The modulus of unseeded empty scaffolds had no effect on T cell proliferation (928±37 at 50Pa and 948±51 MFI at 1345 Pa). MFI was linearly related to cell surface adhesion molecules, specifically ICAM-1, VCAM-1, and integrin α_5 expression ($r^2 = 0.81$, $r^2 = 0.95$, and $r^2 = 0.83$ respectively, Fig. 5b–d).

4. DISCUSSION

Proliferation of many cell types is affected by substrate stiffness. Smooth muscle cells [12] proliferate more quickly on stiff two-dimensional flat substrates, while adult neural stem cells grow best on substrates of intermediate modulus [45]. Fibroblasts and chondrocytes are either not affected by modulus [46], or proliferate better on stiff scaffolds [10,11,42,47]. Effects on cell functionality by alterations in substrate modulus have not been as closely examined. EC are anisotropic cells, in that they have definitive axes of orientation with

respect to flow, adjacent cells and underlying substratum, and most studies to date have examined the effect of substratum rigidity on EC morphology and attachment. The bulk of EC studies use two dimensional culture given the position of EC as vascular epithelium. Those that do consider EC that reside in more complex three dimensional domains have examined 3D culture but focus primarily on tubulogenesis or focal adhesion formation relative to substratum stiffness [37–40]. In this work, we examined the effect of substratum modulus on the biosecretory and cell regulatory functionality of EC in 3D culture, including proliferation, extracellular matrix production, integrin expression, inhibition of smooth muscle cell growth, and immunogenicity. Intriguingly matrix effect followed a distinct pattern in all examined aspects and axes of function – enhancers of proliferation, inflammation, adhesion, and matrix remodeling were all unaffected by modulus while those that down modulate these processes were far more intensely sensitive to stiffness.

We strove to create a set of scaffolds across a wide (27-fold), and physiologically relevant range of moduli while being careful to maintain other matrix and substratum properties. The strut modulus of the unmodified, “base” matrix whose bulk modulus was 173 Pa was measured using the AFM cantilever technique [48] at ~4.4 kPa. Using this value, along with the known bulk moduli of the entire scaffold range, and the assumption that scaffold and strut density were held constant across each scaffold, strut modulus can be estimated to be between ~1.3–34 kPa for the entire range of scaffolds. These values are remarkably akin to the 5–8 kPa modulus of normal vascular media by AFM [4], and close to the 33 kPa modulus of some atherosclerotic plaques[49]. The use of a single, unified “base” scaffold for all studies that was environmentally modified through carbodiimide cross-linking [41,42] or high pressure heating allowed for predictable and consistent modification of modulus while retaining the same matrix physical structure.

EC can stimulate (through secreted growth factors) or inhibit smooth muscle cells (via HSPG), promote or inhibit inflammation and T cell proliferation and cell adhesion by elaboration of cytokines or adhesion molecules, and matrix remodeling through metalloproteinases or their inhibitors. In all of these cases matrix stiffness dictated the elaboration of inhibitory control factors at levels known to exert profound biological effects, but had no effect on the proliferative side of the balance (i.e growth factors and MMPs which are associated with tissue growth and remodeling).

Thus, not only were EC effects on smooth muscle proliferation and EC expression of HSPG modulus-dependent, but dependent in a profoundly correlative manner. The same is true for EC effects on T cells and adhesion molecules such as ICAM-1 and VCAM-1. Immunologically activated ECs express cell surface markers (e.g., MHCII [50,51] and adhesion and costimulatory molecules) which induce proliferation of T cells. Past work has shown that embedding EC in gelatin scaffolds greatly reduces EC-mediated induction of $CD4^+$ T cell proliferation due at least in part to reduced expression of these markers.[29] We show that EC-induced proliferation of $CD4^+$ T cells could be further affected by scaffold modulus. EC cultured on stiff scaffolds induced significantly less T cell proliferation than EC cultured on softer scaffolds. T cell proliferation tracked with VCAM-1 and ICAM-1 expression. The ICAM-1 and VCAM-1 data combined with the T-cell proliferation data suggests that the overall inflammatory state of the EC is reduced when cultured on stiffer scaffolds compared to softer ones.

Clearly, even modest scaffold modulus changes are enough to affect endothelial function. However, the mechanism of this effect is not clear. One possible explanation supported by the data is that the interface between the cells and their substrate is affected by modulus. Even though the underlying substrate provides the physical support for cell growth, the cells do not interact directly with matrix material. Instead, cells sit on extracellular matrix that

they themselves produce. Our data show that EC on softer scaffolds produce significantly more of several common key ECM molecules, including the α_1 and α_5 chains of collagen IV, fibronectin, biglycan and perlecan, than EC on stiffer scaffolds. However, the ratios between these molecules is similar between types of scaffolds, suggesting that while the cells on softer scaffolds are producing *more* matrix than those on softer scaffolds, the ECM itself is biochemically similar. One ECM gene which did not follow this pattern was elastin, which was expressed at higher levels on the stiff substrate than softer ones. Taken together, the data suggest that it might be possible that EC on softer scaffolds may be trying to stiffen their substrate by producing more structural ECM proteins, while cells on stiffer matrices may be trying to achieve the opposite affect by producing more elastin – a molecule which would increase the elasticity of their substrate.

This type of substrate dependent ECM production is found across cell types. It has previously been shown that ECM formation in various cell types is dependent on the material on which they sit. Fibroblasts [52] and embryonic stem cells [53] both produce different ECM when cultured in 2D vs. 3D. Chondrocyte ECM production changes with alterations in 3D structure [54] and with substrate stiffness in 3D [46]. Fibroblasts and EC differentially remodel their ECM in 2D when cultured on substrates of varying stiffness [5]. Finally, EC in vivo differentially express genes for ECM molecules depending on the stiffness of the artery from which they came [21].

Changes in ECM often lead to changes in integrin expression, and in fact, we did find differences between scaffolds of different moduli. $\alpha_5\beta_1$ integrins, which are receptors for fibronectin, one of the ECM proteins most affected by stiffness, were expressed less on cells grown on stiff substrates compared to softer substrates. This was seen both by flow cytometry and at the gene expression level by RT-PCR. These results differ from the results seen for other cell types in the literature. Most studies examining the effect of substrate modulus on integrin and/or focal adhesion expression have found that cells on stiffer substrates tend to produce more of these molecules [14,15,22]. It is possible that in our system, the effect of remodeling in the form of ECM production outweighs the effect of substrate modulus itself in affecting integrin expression. Changes in integrin expression also offer a potential explanation for decreased T cell proliferation with higher modulus scaffolds. We have previously found that blocking expression of integrins $\alpha_5\beta_1$ and $\alpha_v\beta_3$ can lead to decreased endothelial response to immune stimuli in vitro (unpublished data).

Our data allow us to propose a model where changes in scaffold modulus lead to a change in the set-point of the balance between the stimulatory and inhibitory functions of ECs. We can consider an EC in its natural setting to be in balance with the various forces acting on it, including contraction and compression of the vessel, shear stress from blood flow, and the mechanical properties of the substrate/stroma. In the artificial, tissue engineering environment considered here, only substrate mechanical properties are factors. We propose that when one of these forces differs from some “ideal” state, this balance is disturbed, causing the cell to attempt to alter its physical environment to restore balance (Figure 6). In our system, EC attempt to recapitulate the modulus of their natural environment through differential secretion and remodeling of its ECM. This leads to downstream cellular effects, with inhibitory functions affected to a far greater extent than stimulatory signals.

A uniform model of how mechanical forces and substrate physical properties might tie together a wealth of emerging data on EC function in complex environments. Future work will focus on confirming and extending the proposed model. Additionally, we will attempt to determine if changes in ECM and integrin expression are the driving force behind the differences in EC function seen with alterations in modulus, or if there is another mechanism at play. Work will be conducted to determine which pathways are involved in regulation of

ECM deposition and integrin expression in response to change in scaffold modulus. Potential targets include the TGF-β1, NFκB and MAP kinase pathways, all of which respond at least in part to changes in mechanical forces [55,56]. The differential regulation by substratum modulus of inhibitory and stimulatory biosecretory regulatory aspects of the EC remains a fascinating finding deserving of further investigation and elucidation.

5. CONCLUSIONS

Endothelial cells possess distinct anatomic, phenotypic, sensory, regulatory and biochemical states. We now show how variation in one aspect affects the others, especially in three-dimensional environments. Substrate mechanics have long been known to affect endothelial cell function, though data in three-dimensional systems has been limited. We now show that even modest changes in substrate modulus affect endothelial cell biology including growth, regulation of smooth muscle cell proliferation, and immunomodulation, and that the endothelial cell seeks homeostasis through continued remodeling of its substratum. Mechanical forces induce endothelial cells to affect extracellular matrix production and integrin expression to, in turn, restore the substratum mechanical set point. Moreover, the endothelial secretome is variably sensitive to changes in substratum - with inhibitory endothelial cell regulatory functions far more sensitive to substratum than the stimulatory signals of the regulatory axis. These findings will be appreciated as increasingly significant as we continue to discover endogenous three-dimensional niches for endothelial cells and their progenitors and as the potential of tissue-engineered endothelial constructs is realized.

Supplementary Material

Refer to Web version on PubMed Central for supplementary material.

Acknowledgments

Funding for this work was provided by the NIH (R01 GM49039) and the Else Kröner-Fresenius Stiftung (P36/07// A45/07, to Heiko Methe)

References

1. Yeung T, Georges PC, Flanagan LA, Marg B, Ortiz M, Funaki M, et al. Effects of substrate stiffness on cell morphology, cytoskeletal structure, and adhesion. Cell Motil Cytoskeleton. 2005; 60:24–34. [PubMed: 15573414]
2. Lo CM, Wang HB, Dembo M, Wang YL. Cell movement is guided by the rigidity of the substrate. Biophys J. 2000; 79:144–52. [PubMed: 10866943]
3. Engler A, Bacakova L, Newman C, Hategan A, Griffin M, Discher D. Substrate compliance versus ligand density in cell on gel responses. Biophys J. 2004; 86:617–28. [PubMed: 14695306]
4. Engler AJ, Richert L, Wong JY, Picart C, Discher DE. Surface probe measurements of the elasticity of sectioned tissue, thin gels and polyelectrolyte multilayer films: Correlations between substrate stiffness and cell adhesion. Surface Science. 2004; 570:142–54.
5. Gray DS, Tien J, Chen CS. Repositioning of cells by mechanotaxis on surfaces with micropatterned Young's modulus. J Biomed Mater Res A. 2003; 66:605–14. [PubMed: 12918044]
6. Peyton SR, Putnam AJ. Extracellular matrix rigidity governs smooth muscle cell motility in a biphasic fashion. J Cell Physiol. 2005; 204:198–209. [PubMed: 15669099]
7. Smith JT, Elkin JT, Reichert WM. Directed cell migration on fibronectin gradients: effect of gradient slope. Exp Cell Res. 2006; 312:2424–32. [PubMed: 16730349]
8. Pelham RJ Jr, Wang Y. Cell locomotion and focal adhesions are regulated by substrate flexibility. Proc Natl Acad Sci USA. 1997; 94:13661–5. [PubMed: 9391082]
9. Giannone G, Sheetz MP. Substrate rigidity and force define form through tyrosine phosphatase and kinase pathways. Trends Cell Biol. 2006; 16:213–223. [PubMed: 16529933]

10. Subramanian A, Lin H-Y. Crosslinked chitosan: its physical properties and the effects of matrix stiffness on chondrocyte cell morphology and proliferation. J Biomed Mater Res A. 2005; 75:742–53. [PubMed: 16110496]
11. Wang HB, Dembo M, Wang YL. Substrate flexibility regulates growth and apoptosis of normal but not transformed cells. Am J Physiol, Cell Physiol. 2000; 279:C1345–50. [PubMed: 11029281]
12. Peyton SR, Raub CB, Keschrumrus VP, Putnam AJ. The use of poly(ethylene glycol) hydrogels to investigate the impact of ECM chemistry and mechanics on smooth muscle cells. Biomaterials. 2006; 27:4881–93. [PubMed: 16762407]
13. Semler EJ, Lancin PA, Dasgupta A, Moghe PV. Engineering hepatocellular morphogenesis and function via ligand-presenting hydrogels with graded mechanical compliance. Biotechnol Bioeng. 2005; 89:296–307. [PubMed: 15744840]
14. Paszek MJ, Zahir N, Johnson KR, Lakins JN, Rozenberg GI, Gefen A, et al. Tensional homeostasis and the malignant phenotype. Cancer Cell. 2005; 8:241–54. [PubMed: 16169468]
15. Flanagan LA, Ju Y-E, Marg B, Osterfield M, Janmey PA. Neurite branching on deformable substrates. Neuroreport. 2002; 13:2411–5. [PubMed: 12499839]
16. Hayoz D, Brunner HR. Remodelling of conduit arteries in hypertension: special emphasis on the mechanical and metabolic consequences of vascular hypertrophy. Blood Press Suppl. 1997; 2:39–42. [PubMed: 9495625]
17. Korshunov VA, Schwartz SM, Berk BC. Vascular remodeling: hemodynamic and biochemical mechanisms underlying Glagov's phenomenon. Arterioscler Thromb Vasc Biol. 2007; 27:1722–8. [PubMed: 17541029]
18. Nugent MA, Karnovsky MJ, Edelman ER. Vascular cell-derived heparan sulfate shows coupled inhibition of basic fibroblast growth factor binding and mitogenesis in vascular smooth muscle cells. Circ Res. 1993; 73:1051–60. [PubMed: 8222077]
19. Parikh SA, Edelman ER. Endothelial cell delivery for cardiovascular therapy. Adv Drug Deliv Rev. 2000; 42:139–61. [PubMed: 10942819]
20. Rogers C, Parikh S, Seifert P, Edelman ER. Endogenous cell seeding. Remnant endothelium after stenting enhances vascular repair. Circulation. 1996; 94:2909–14. [PubMed: 8941120]
21. Durier S, Fassot C, Laurent S, Boutouyrie P, Couetil J-P, Fine E, et al. Physiological genomics of human arteries: quantitative relationship between gene expression and arterial stiffness. Circulation. 2003; 108:1845–51. [PubMed: 14530203]
22. Wallace CS, Strike SA, Truskey GA. Smooth muscle cell rigidity and extracellular matrix organization influence endothelial cell spreading and adhesion formation in coculture. Am J Physiol Heart Circ Physiol. 2007; 293:H1978–86. [PubMed: 17644568]
23. Ohya S, Kidoaki S, Matsuda T. Poly(N-isopropylacrylamide) (PNIPAM)-grafted gelatin hydrogel surfaces: interrelationship between microscopic structure and mechanical property of surface regions and cell adhesiveness. Biomaterials. 2005; 26:3105–11. [PubMed: 15603805]
24. Nugent HM, Edelman ER. Endothelial implants provide long-term control of vascular repair in a porcine model of arterial injury. J Surg Res. 2001; 99:228–34. [PubMed: 11469891]
25. Nugent HM, Rogers C, Edelman ER. Endothelial implants inhibit intimal hyperplasia after porcine angioplasty. Circ Res. 1999; 84:384–91. [PubMed: 10066672]
26. Nugent HM, Groothuis A, Seifert P, Guerraro JL, Nedelman M, Mohanakumar T, et al. Perivascular endothelial implants inhibit intimal hyperplasia in a model of arteriovenous fistulae: a safety and efficacy study in the pig. J Vasc Res. 2002; 39:524–33. [PubMed: 12566978]
27. Nugent HM, Sjin RTT, White D, Milton LG, Manson RJ, Lawson JH, et al. Adventitial endothelial implants reduce matrix metalloproteinase-2 expression and increase luminal diameter in porcine arteriovenous grafts. J Vasc Surg. 2007; 46:548–56. [PubMed: 17826244]
28. Therapeutic Applications | Pervasis [Internet]. [cited 2011]. Available from: http://www.pervasistx.com/clinical-development/therapeutic-applications
29. Methe H, Nugent HM, Groothuis A, Seifert P, Sayegh MH, Edelman ER. Matrix embedding alters the immune response against endothelial cells in vitro and in vivo. Circulation. 2005; 112:I89–95. [PubMed: 16159871]
30. Methe H, Edelman ER. Cell-matrix contact prevents recognition and damage of endothelial cells in states of heightened immunity. Circulation. 2006; 114:I233–8. [PubMed: 16820578]

31. Hess S, Methe H, Kim J-O, Edelman ER. NF-kappaB activity in endothelial cells is modulated by cell substratum interactions and influences chemokine-mediated adhesion of natural killer cells. Cell Transplant. 2009; 18:261–73. [PubMed: 19558775]
32. Methe H, Hess S, Edelman ER. Endothelial cell-matrix interactions determine maturation of dendritic cells. Eur J Immunol. 2007; 37:1773–84. [PubMed: 17559179]
33. Methe H, Groothuis A, Sayegh MH, Edelman ER. Matrix adherence of endothelial cells attenuates immune reactivity: induction of hyporesponsiveness in allo- and xenogeneic models. FASEB J. 2007; 21:1515–26. [PubMed: 17264166]
34. Methe H, Hess S, Edelman ER. The effect of three-dimensional matrix-embedding of endothelial cells on the humoral and cellular immune response. Semin Immunol. 2008; 20:117–22. [PubMed: 18243732]
35. Conte MS, Nugent HM, Gaccione P, Guleria I, Roy-Chaudhury P, Lawson JH. Multicenter phase I/II trial of the safety of allogeneic endothelial cell implants after the creation of arteriovenous access for hemodialysis use: the V-HEALTH study. J Vasc Surg. 2009; 50:1359–68.e1. [PubMed: 19958986]
36. Franses JW, Baker AB, Chitalia VC, Edelman ER. Stromal endothelial cells directly influence cancer progression. Sci Transl Med. 2011; 3:66ra5.
37. Sieminski AL, Hebbel RP, Gooch KJ. The relative magnitudes of endothelial force generation and matrix stiffness modulate capillary morphogenesis in vitro. Exp Cell Res. 2004; 297:574–84. [PubMed: 15212957]
38. Sieminski AL, Was AS, Kim G, Gong H, Kamm RD. The stiffness of three-dimensional ionic self-assembling peptide gels affects the extent of capillary-like network formation. Cell Biochem Biophys. 2007; 49:73–83. [PubMed: 17906362]
39. Deroanne CF, Lapiere CM, Nusgens BV. In vitro tubulogenesis of endothelial cells by relaxation of the coupling extracellular matrix-cytoskeleton. Cardiovasc Res. 2001; 49:647–58. [PubMed: 11166278]
40. Yamamura N, Sudo R, Ikeda M, Tanishita K. Effects of the mechanical properties of collagen gel on the in vitro formation of microvessel networks by endothelial cells. Tissue Eng. 2007; 13:1443–53. [PubMed: 17518745]
41. Harley BA, Leung JH, Silva ECCM, Gibson LJ. Mechanical characterization of collagen-glycosaminoglycan scaffolds. Acta Biomater. 2007; 3:463–74. [PubMed: 17349829]
42. Lee CR, Grodzinsky AJ, Spector M. The effects of cross-linking of collagen-glycosaminoglycan scaffolds on compressive stiffness, chondrocyte-mediated contraction, proliferation and biosynthesis. Biomaterials. 2001; 22:3145–54. [PubMed: 11603587]
43. Johnson KR, Leight JL, Weaver VM. Demystifying the effects of a three-dimensional microenvironment in tissue morphogenesis. Methods Cell Biol. 2007; 83:547–83. [PubMed: 17613324]
44. Farndale RW, Buttle DJ, Barrett AJ. Improved quantitation and discrimination of sulphated glycosaminoglycans by use of dimethylmethylene blue. Biochim Biophys Acta. 1986; 883:173–7. [PubMed: 3091074]
45. Leipzig ND, Shoichet MS. The effect of substrate stiffness on adult neural stem cell behavior. Biomaterials. 2009; 30:6867–78. [PubMed: 19775749]
46. Vickers SM, Squitieri LS, Spector M. Effects of cross-linking type II collagen-GAG scaffolds on chondrogenesis in vitro: dynamic pore reduction promotes cartilage formation. Tissue Eng. 2006; 12:1345–55. [PubMed: 16771647]
47. Hadjipanayi E, Mudera V, Brown RA. Close dependence of fibroblast proliferation on collagen scaffold matrix stiffness. J Tissue Eng Regen Med. 2009; 3:77–84. [PubMed: 19051218]
48. Silva ECCM, Tong L, Yip S, Van Vliet KJ. Size effects on the stiffness of silica nanowires. Small. 2006; 2:239–43. [PubMed: 17193028]
49. Barrett SRH, Sutcliffe MPF, Howarth S, Li Z-Y, Gillard JH. Experimental measurement of the mechanical properties of carotid atherothrombotic plaque fibrous cap. J Biomech. 2009; 42:1650–5. [PubMed: 19464014]

50. Dorling A, Binns R, Lechler RI. Significant primary indirect human T-cell anti-pig xenoresponses observed using immature porcine dendritic cells and SLA-class II-negative endothelial cells. Transplant Proc. 1996; 28:654. [PubMed: 8623327]
51. Vallée I, Guillaumin JM, Thibault G, Gruel Y, Lebranchu Y, Bardos P, et al. Human T lymphocyte proliferative response to resting porcine endothelial cells results from an HLA-restricted, IL-10-sensitive, indirect presentation pathway but also depends on endothelial-specific costimulatory factors. J Immunol. 1998; 161:1652–8. [PubMed: 9712027]
52. Webb K, Li W, Hitchcock RW, Smeal RM, Gray SD, Tresco PA. Comparison of human fibroblast ECM-related gene expression on elastic three-dimensional substrates relative to two-dimensional films of the same material. Biomaterials. 2003; 24:4681–90. [PubMed: 12951011]
53. Liu H, Lin J, Roy K. Effect of 3D scaffold and dynamic culture condition on the global gene expression profile of mouse embryonic stem cells. Biomaterials. 2006; 27:5978–89. [PubMed: 16824594]
54. Yamane S, Iwasaki N, Kasahara Y, Harada K, Majima T, Monde K, et al. Effect of pore size on in vitro cartilage formation using chitosan-based hyaluronic acid hybrid polymer fibers. J Biomed Mater Res A. 2007; 81:586–93. [PubMed: 17177288]
55. Baker AB, Ettenson DS, Jonas M, Nugent MA, Iozzo RV, Edelman ER. Endothelial cells provide feedback control for vascular remodeling through a mechanosensitive autocrine TGF-beta signaling pathway. Circ Res. 2008; 103:289–97. [PubMed: 18583708]
56. Lehoux S, Castier Y, Tedgui A. Molecular mechanisms of the vascular responses to haemodynamic forces. J Intern Med. 2006; 259:381–92. [PubMed: 16594906]

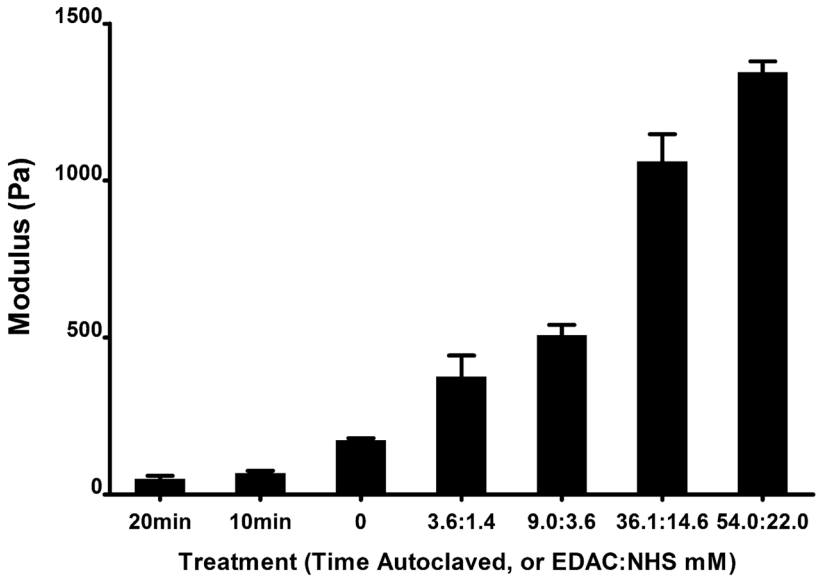

Figure 1. Scaffold Modulus vs. Crosslinking/121C, 20mmHgTreatment

Scaffold stiffness was characterized by uniaxial compression, at a rate of 0.01mm/s, of 12mm scaffold disks in PBS using a Zwick mechanical tester. Young's modulus was calculated as the slope of the linear region of the resulting stress strain curve. All error bars are ± SEM.

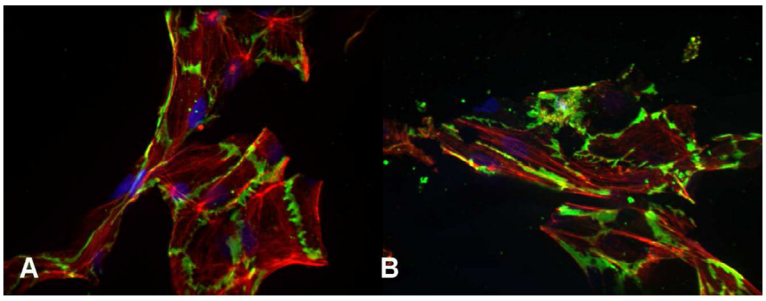

Figure 2.

EC retain a normal, cobble-stone appearance on scaffolds of varying modulus. All cells show a normal immuno-fluorescent pattern of EC markers, including CD31 (green). Actin (red) stress fibers are visible on all scaffold types. *Left:* 50Pa scaffold *Right:* 1345Pa scaffold

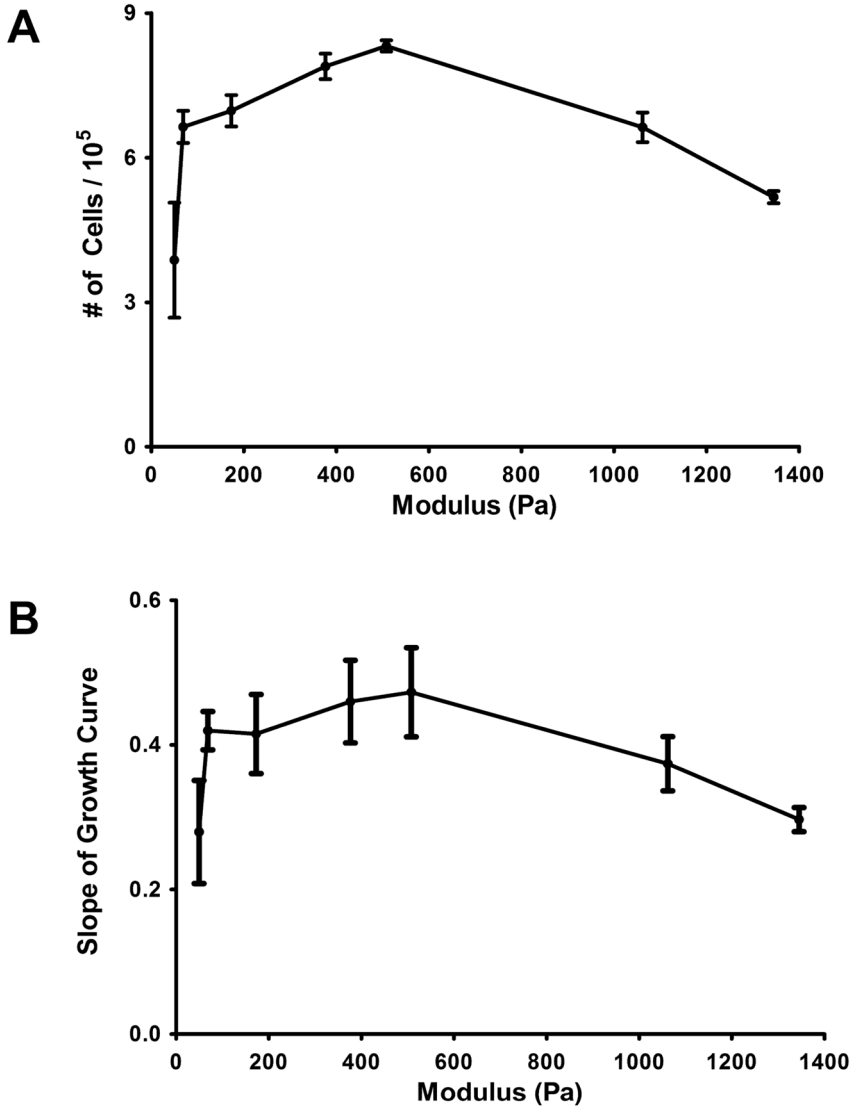

Figure 3. Endothelial Cell Growth is Dependent on Scaffold Modulus

Top: Cell per scaffold at day 21 (confluence) vs. modulus. Cell number peaks at 508Pa and falls off at both lower and higher moduli. Error bars are mean cell number ± SEM. *Bottom:* EC growth rate, as measured by slope of growth curve between days 5–21. As with cell number, growth rate peaks at 508Pa and falls at lower and higher moduli. Error bars represent standard error of linear regression to cell number data.

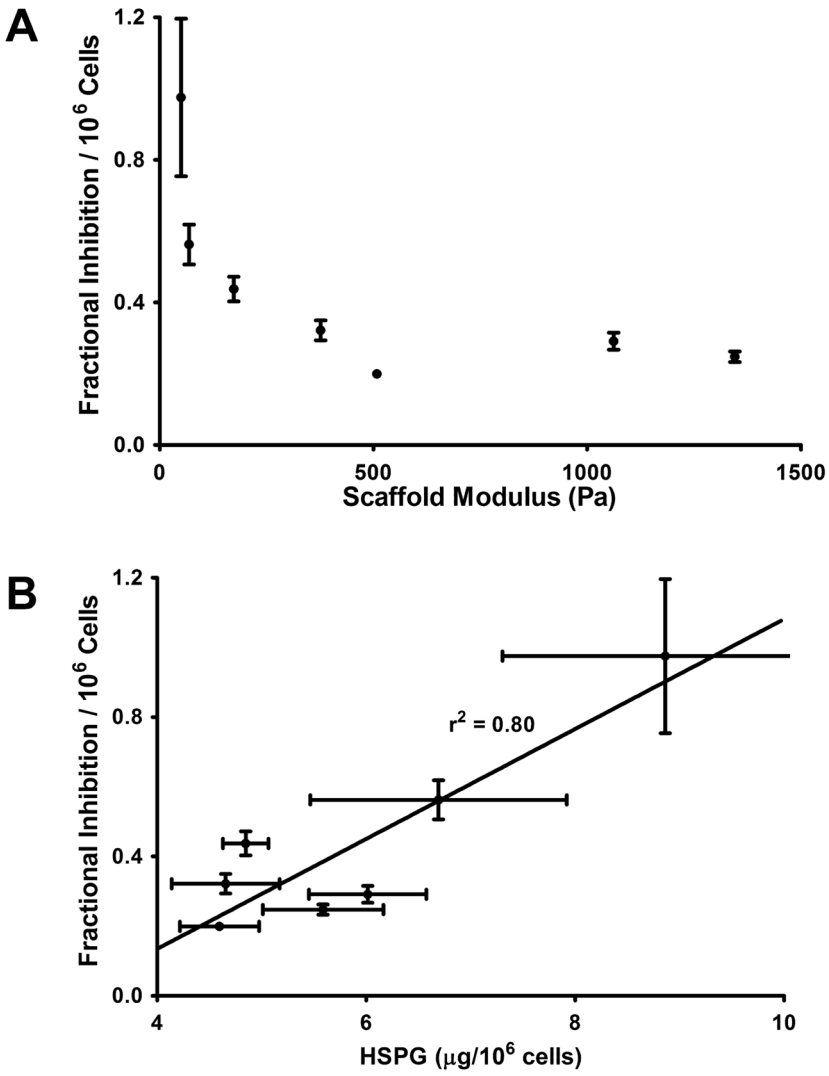

Figure 4. Smooth Muscle Cell Growth Inhibition and Heparan Sulfate Proteoglycan Secretion Are Affected by Scaffold Modulus

Top) Inhibition of smooth muscle cell growth by EC is related to scaffold modulus. Bottom) Inhibition and HSPG secretion are linearly related. Correlation $r^2 = 0.80$, $p < 0.001$. All error bars are ± SEM.

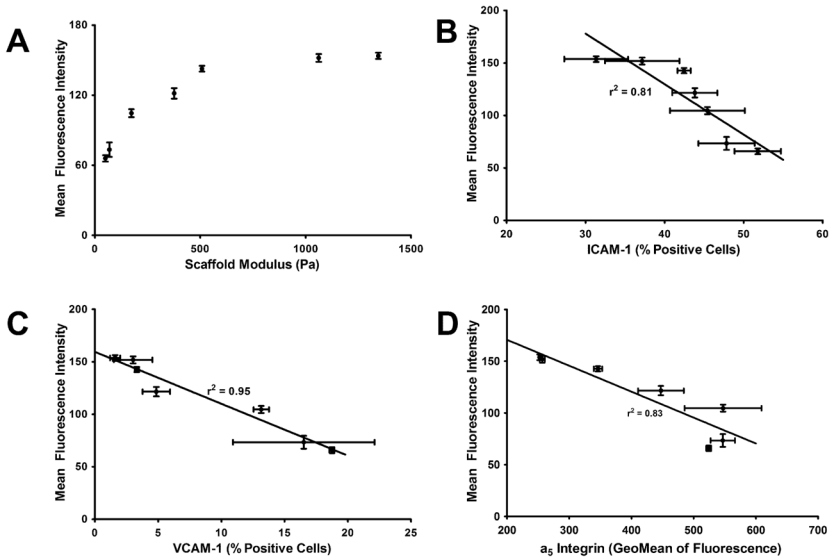

Figure 5. Endothelial Cell Induced T-Cell Proliferation

Top: MFI (inversely related to T-cell proliferation) increases with scaffold modulus, indicating decreased proliferation at higher modulus. (*left)* MFI is linearly related to endothelial α_5 integrin expression, $r^2 = 0.83$. (*right*) ***Bottom***: MFI is linearly related to endothelial ICAM-1 ($r^2 = 0.81$) (*left*) and VCAM-1 ($r^2 = 0.95$) (*right*) expression. All error bars are ± SEM.

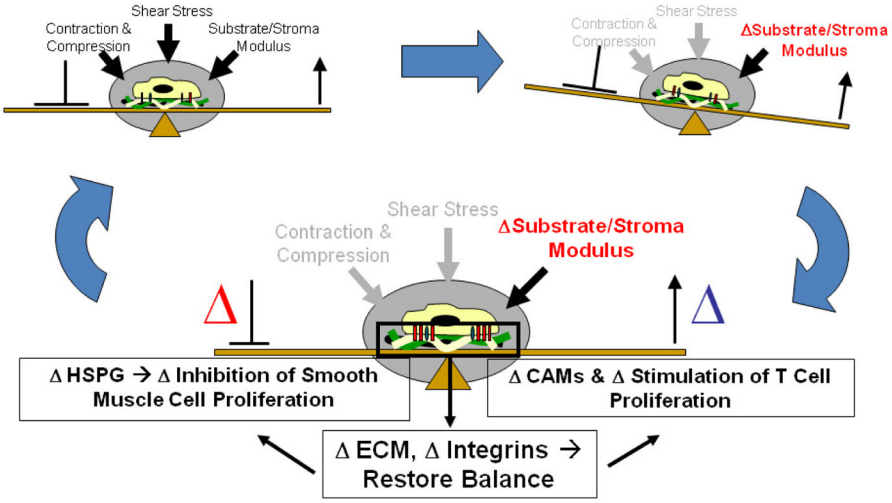

Figure 6. Proposed Model for Mechanism of Modulus Effect on Endothelial Cell Function

Upper Left: In a natural environment, external forces on the cell are in balance and the cell carries out its normal inhibitory and stimulatory functions. *Upper Right:* When substrate modulus is changed, the balance is disrupted. *Bottom:* In order to restore balance of external forces, the cell alters ECM production and integrin expression, leading to changes in cell function.